

SIMULTANEOUS OBSERVATION OF A MORETON WAVE ON 1997 NOVEMBER 3 IN H α AND SOFT X-RAYS

N. NARUKAGE,¹ H. S. HUDSON,² T. MORIMOTO,¹ S. AKIYAMA,^{1,3} R. KITAI,¹ H. KUROKAWA,¹ AND K. SHIBATA¹

Received 2002 February 16; accepted 2002 May 6; published 2002 May 20

ABSTRACT

We report the observation of a Moreton wave in H α (line center and $\pm 0.8 \text{ \AA}$) with the Flare Monitoring Telescope at the Hida Observatory of Kyoto University at 4:36–4:41 UT on 1997 November 3. The same region (NOAA Active Region 8100) was simultaneously observed in soft X-rays with the soft X-ray telescope on board *Yohkoh*, and a wavelike disturbance (“X-ray wave”) was also found. The position of the wave front as well as the direction of propagation of the X-ray wave roughly agree with those of the Moreton wave. The propagation speeds of the Moreton wave and the X-ray wave are about 490 ± 40 and $630 \pm 100 \text{ km s}^{-1}$, respectively. Assuming that the X-ray wave is an MHD fast-mode shock, we can estimate the propagation speed of the shock, on the basis of MHD shock theory and the observed soft X-ray intensities ahead of and behind the X-ray wave front. The estimated fast shock speed is $400\text{--}760 \text{ km s}^{-1}$, which is in rough agreement with the observed propagation speed of the X-ray wave. The fast-mode Mach number of the X-ray wave is also estimated to be about 1.15–1.25. These results suggest that the X-ray wave is a weak MHD fast-mode shock propagating through the corona and hence is the coronal counterpart of the Moreton wave.

Subject headings: shock waves — Sun: chromosphere — Sun: corona — Sun: flares — Sun: magnetic fields

1. INTRODUCTION

Moreton waves are flare-associated waves observed to propagate across the solar disk in H α , especially in the wing of H α (Moreton 1960; Smith & Harvey 1971). They propagate at speeds of $500\text{--}1500 \text{ km s}^{-1}$ with arclike fronts in somewhat restricted angles and are often associated with type II radio bursts (Kai 1969) and coronal EIT waves (Thompson et al. 2000; Klassen et al. 2000; Warmuth et al. 2001). The Moreton wave has been identified as the intersection of a coronal MHD fast-mode weak shock wave and the chromosphere (Uchida 1968, 1970; Uchida, Altschuler, & Newkirk 1973). However, the generation mechanism of a Moreton wave has not been made clear yet.

Recently, the soft X-ray telescope (SXT) on board *Yohkoh* discovered wavelike disturbances in the solar corona associated with flares (Khan & Hudson 2000), which we call “X-ray waves” in this Letter. The first simultaneous observation of a Moreton wave and an X-ray wave was reported by Khan & Aurass (2002). In this Letter, we report a second example. Interestingly, our event and the Khan-Aurass event were observed on the same day (1997 November 3) in the same region (NOAA Active Region 8100) but at different times (04:32 and 09:04, respectively). The next day, another Moreton wave occurred in this region (Eto et al. 2002).

The purpose of this Letter is to examine the basic question of whether the X-ray wave is the coronal counterpart of the Moreton wave, i.e., a coronal MHD fast-mode shock, based on MHD shock theory and *Yohkoh*/SXT soft X-ray images. The result shows that the observed properties of the X-ray wave are consistent with the wave interpreted as a coronal MHD fast-mode weak shock.

In § 2, the instrumentation and observing methods are summarized. In § 3, the results of the analysis of the Moreton wave and the X-ray wave are described. In § 4, a summary and a discussion are given.

2. OBSERVATIONS

In this Letter, we study two kinds of flare-associated waves: the chromospheric Moreton wave and coronal X-ray wave associated with a C-class flare in NOAA AR 8100 at S20°, W13° on 1997 November 3. The flare started at 04:32 UT and peaked at 04:38 (*GOES* times).

The Moreton wave was observed in H α (line center and $\pm 0.8 \text{ \AA}$) with the Flare Monitoring Telescope (FMT; Kurokawa et al. 1995) at the Hida Observatory of Kyoto University. The FMT observes four full-disk images (in the H α line center and $\pm 0.8 \text{ \AA}$ and continuum) and one solar limb image (in the H α line center). We use the full-disk images in H α $+0.8 \text{ \AA}$, because a Moreton wave front is best seen in the red wing of the H α line (H α $+0.8 \text{ \AA}$). This is because the mass motion at the wave front is downward when the front enters the chromosphere. The time resolution of the images used in this Letter is 1 minute, although the FMT operates at a higher time resolution. The pixel size is $4''2$.

The X-ray wave was observed in soft X-rays with *Yohkoh*/SXT (Tsuneta et al. 1991). The SXT is sensitive to soft X-ray photons in the energy range $\sim 0.28\text{--}4 \text{ keV}$, which corresponds to wavelengths $\sim 3\text{--}45 \text{ \AA}$. In this Letter, we use partial frame images observed with the AlMg filter. The observing time cadence is about 50 s. The pixel sizes of the half- and quarter-resolution images are $4''91$ and $9''82$, respectively.

The magnetic field of the photosphere was observed with the Michelson Doppler Imager (MDI; Scherrer et al. 1995) on board the *Solar and Heliospheric Observatory* (*SOHO*). The time resolution and pixel sizes are about 90 minutes and $2''$, respectively.

3. RESULTS

Figure 1 shows the observed images on 1997 November 3 of NOAA AR 8100. Figures 1a–1f are “running difference” images (where each image has the previous image subtracted from it) observed in H α $+0.8 \text{ \AA}$. The running difference method clearly shows the motion of the Moreton wave. Figures 1g–1j are the direct soft X-ray images (*middle panels*) and running difference images (*bottom panels*). In Figure 1k, the

¹ Kwasan and Hida Observatories, Kyoto University, Yamashina, Kyoto 607-8471, Japan; naru@kwasan.kyoto-u.ac.jp.

² Solar Physics Research Corporation, Sagamihara, Kanagawa 229-8510, Japan.

³ Present address: Naval Research Laboratory, 4555 Overlook Avenue, SW, Washington, DC 20375-5320.

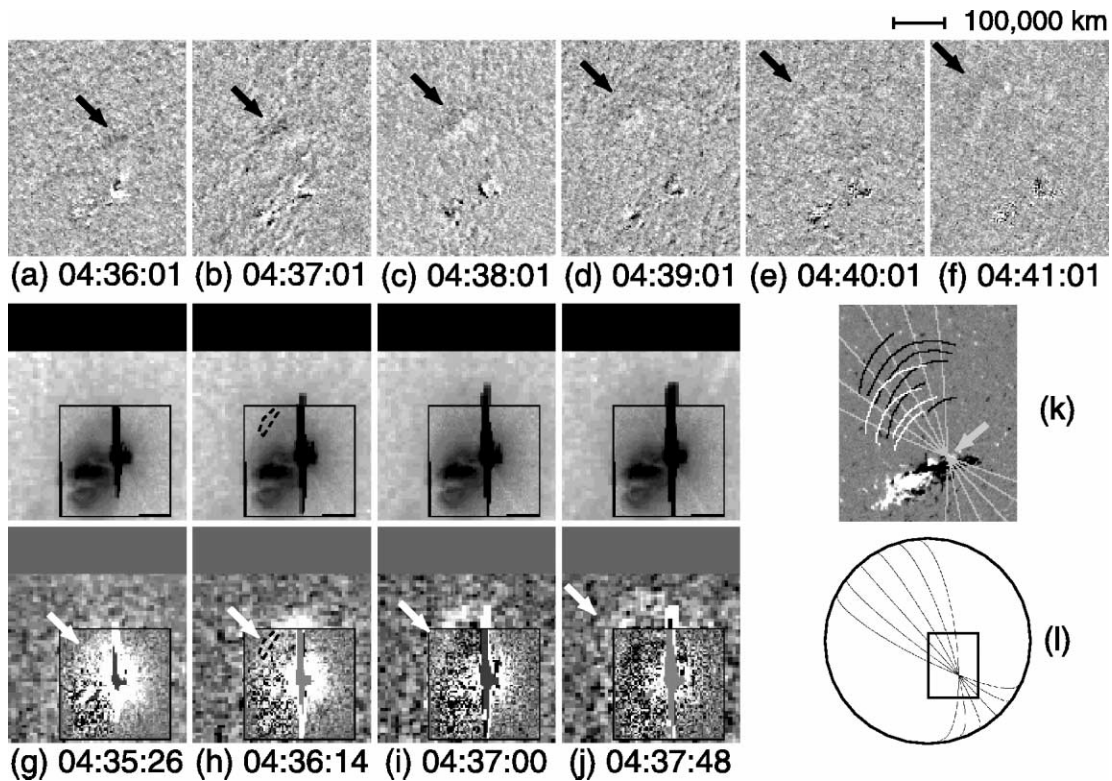


FIG. 1.—Observed images on 1997 November 3 at NOAA AR 8100. (a–f) H α +0.8 Å running difference images of a Moreton wave (*black arrows*). (g–j) Soft X-ray (*middle panels*) and running difference (*bottom panels*) images of an X-ray wave (*white arrows*) taken with the AIMG filter. The images inside and outside the boxes are half-resolution (4.91) and quarter-resolution (9.82) images, respectively. (k) Wave fronts of the Moreton wave at every minute from 04:36:01 to 04:41:01 UT (*black lines*) and the X-ray wave at 04:35:26, 04:36:14, 04:37:00, and 04:37:48 UT (*white lines*) overlaid on the photospheric magnetic field observed at 04:51:04. Gray lines show the great circles through the flare site (*gray arrow*). The rectangle, circle, and lines shown in (l) are the field of view of (a)–(k), the limb of the Sun, and the great circles, respectively.

apparent positions of the wave fronts are overlaid on the longitudinal magnetogram from MDI. Using the running difference images, the Moreton wave (*black lines*) can be identified visually from 04:36:01 to 04:41:01 UT, and the X-ray wave (*white lines*) from 04:35:26 to 04:37:48 UT. Both propagate roughly in the same direction and agree approximately in location. The field of view is illustrated by the box in Figure 1l.

In Figure 2, the distances of the wave fronts from the flare site along the great circles are plotted. We assume the brightest region is the flare site. The propagation speeds of the Moreton wave and the X-ray wave are roughly constant at 490 ± 40 and 630 ± 100 km s $^{-1}$, respectively, using the scatter of points from the four great circles as a measure. In fact, the Moreton wave seems to be somewhat decelerating. The positions refer to the leading edge of the wave front rather than to the peak.

4. DISCUSSION

In the model of Uchida (1968, 1970; Uchida et al. 1973), a Moreton wave is the sweeping skirt on the chromosphere of a weak MHD fast-mode shock that propagates in the corona. This model thus also explains the meter-wave type II radio burst as a signature of the coronal propagation and predicts the existence of a coronal counterpart of the chromospheric Moreton wave. In fact, in our event, the position of the wave front as well as the direction of propagation of the X-ray wave roughly agree with those of the Moreton wave (Fig. 1k).

Let us now examine whether the X-ray wave is an MHD fast-mode shock (hereafter simply called a fast shock), i.e., the coronal counterpart of the Moreton wave. Assuming that the

X-ray wave is a fast shock, we can estimate its propagation speed, based on MHD shock theory and the observed soft X-ray intensities ahead of and behind the X-ray wave front. If this estimated speed of the shock is consistent with the observed propagation speed of the X-ray wave, we can conclude that the X-ray wave is a fast shock.

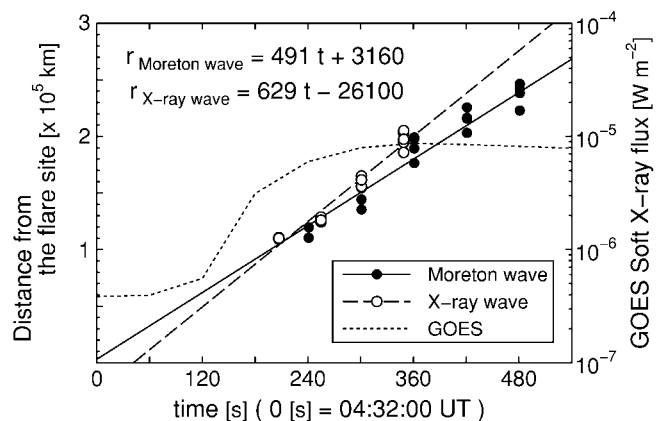


FIG. 2.—Propagation of the Moreton wave (*filled circles*) and the X-ray wave (*open circles*). First-degree polynomial fits of the Moreton wave (*solid line*) and the X-ray wave (*dashed line*) are shown. The propagation speeds of the Moreton wave and the X-ray wave are 490 ± 40 and 630 ± 100 km s $^{-1}$, respectively. The dotted line shows the soft X-ray flux observed by the GOES 9 satellite.

The jump condition of MHD shock theory (Priest 1982), for

$$X \equiv \frac{\rho_2}{\rho_1}, \quad (1)$$

gives

$$\begin{aligned} & (v_1^2 - Xv_{A1}^2)^2 \{Xc_{s1}^2 + \frac{1}{2}v_1^2 \cos^2 \theta_1 [X(\gamma - 1) - (\gamma + 1)]\} \\ & + \frac{1}{2}v_{A1}^2 v_1^2 \sin^2 \theta_1 X \\ & \times \{[\gamma + X(2 - \gamma)]v_1^2 - Xv_{A1}^2 [(\gamma + 1) - X(\gamma - 1)]\} = 0, \end{aligned} \quad (2)$$

$$\frac{v_{2x}}{v_{1x}} = X^{-1}, \quad (3)$$

$$\frac{v_{2y}}{v_{1y}} = \frac{v_1^2 - v_{A1}^2}{v_1^2 - Xv_{A1}^2}, \quad (4)$$

$$\frac{p_2}{p_1} = X + \frac{(\gamma - 1)Xv_1^2}{2c_{s1}^2} \left(1 - \frac{v_2^2}{v_1^2}\right), \quad (5)$$

$$\frac{T_2}{T_1} = \frac{p_2/p_1}{\rho_2/\rho_1} = \frac{p_2/p_1}{X}. \quad (6)$$

Here the quantities ahead of the shock are denoted by 1 and those behind by 2, in a frame of reference moving with the shock. In equation (2), v_{A1} is the Alfvén velocity [$=B_1/(\mu_0\rho_1)^{1/2}$], c_{s1} the sound speed, given as $(\gamma p_1/\rho_1)^{1/2} = (\gamma RT_1/\bar{\mu})^{1/2}$, where $\bar{\mu}$ is the mean atomic weight (taken as 0.6 in this Letter; Priest 1982), γ the ratio of specific heats ($=5/3$ in this Letter), and θ_1 the inclination of the upstream magnetic field to the shock normal (the x -axis). The y -axis is taken to be perpendicular to the shock normal, such that the magnetic field and velocity vectors are in the x - y plane. There are three solutions for v_1 from equation (2), among which the largest corresponds to the fast-mode shock. In the limit of $\theta_1 \rightarrow 90^\circ$, the shock becomes perpendicular. Using these six equations, the quantities ahead of the shock ($\rho_1, T_1, B_1, \theta_1, v_1$) determine those behind ($\rho_2, T_2, B_2, \theta_2, v_2$).

In the simplest approximation, the soft X-ray intensity is proportional to the square of the plasma density and an instrument-specific function of the temperature,

$$I_x = n^2 l f(T) \propto \rho^2 f(T), \quad (7)$$

where I_x is the soft X-ray intensity, n is the plasma number density, l is the line-of-sight plasma scale, and $f(T)$ represents the plasma emissivity and the filter response (Tsuneta et al. 1991). Hence, the above can be rewritten such that $(I_{x1}, T_1, B_1, \theta_1, v_1)$ determine $(I_{x2}, T_2, B_2, \theta_2, v_2)$. In other words, if we know $(I_{x1}, T_1, B_1, \theta_1, I_{x2})$, we can find $(v_1, T_2, B_2, \theta_2, v_2)$. (See the Appendix and Fig. 3 for a different approach.) The physical parameters ahead of the shock (i.e., in region 1), such as temperature (T_1)

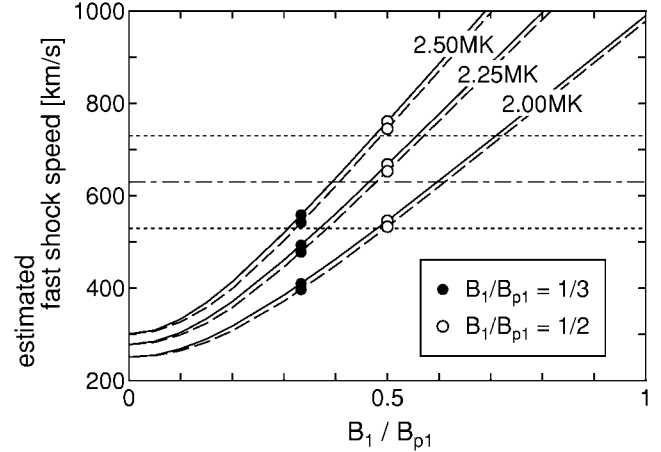


Fig. 3.—Estimated perpendicular (solid lines) and oblique (dashed lines) shock speeds. B_1 and B_{p1} are the coronal and photospheric magnetic field strengths, respectively. The dot-dashed and dotted lines show the observed propagation speeds of the X-ray wave (630 km s^{-1}) and the error bar ($\pm 100 \text{ km s}^{-1}$), respectively.

and density (ρ_1) are obtained from the preflare images and the filter ratio method (Tsuneta et al. 1991). The coronal magnetic field strength (B_1) is derived from the MDI images.

We have four images of the X-ray wave (Figs. 1g–1j), but three of them are inappropriate for analysis. The wave front in Figure 1g is too near the flare site and too greatly influenced by scattered light from the flare. The intensities of the wave fronts in Figures 1i and 1j are too low, so we cannot distinguish the real signal from noise. We analyze a single image, Figure 1h, observed at 04:36:14.

We measure I_{x1} and I_{x2} and obtain $I_{x2}/I_{x1} = 3.27$, where the intensities of the X-ray wave are measured in the area encircled by a dashed line in Figure 1h. The value of T_1 is calculated using preflare full-frame images taken with the thin Al and AlMg filters of SXT as $T_1 = 2.25 \pm 0.25 \text{ MK}$. Substituting this T_1 into the SXT response function gives the emission measure. We calculate the density (ρ_1) assuming that the line-of-sight distance (l) of the observed region is the coronal pressure scale height [$(1.00 - 1.26) \times 10^5 \text{ km}$ for 2.00–2.50 MK]. The photospheric magnetic field strength (B_{p1}) was observed by MDI, and we assume that the coronal magnetic field strength (B_1) is one-third or one-half of B_{p1} . This assumption is justified from a different approach discussed in the Appendix and Figure 3. When $\theta_1 = 90^\circ$, the shock is perpendicular, and $\theta_1 = 60^\circ$ corresponds to an oblique shock. Using equations (1)–(7), these observational properties give the propagation speed of the shock ($v_{sh} = v_{1x} = v_1 \cos \theta_1$) as shown in Table 1.

The estimated fast-shock speed, 400–760 km s^{-1} , is in rough agreement with the observed propagation speed of the X-ray wave, $630 \pm 100 \text{ km s}^{-1}$. The fast-mode Mach number of the X-ray wave is consistent with values in the range of 1.15–1.25. These results suggest that the X-ray wave is a fast shock propagating through the corona and hence is the coronal counterpart of the Moreton wave.

From Figure 1k, we see that the position of the wave front as well as the direction of propagation of the X-ray wave roughly agree with those of the Moreton wave, although the exact positions and speeds are different. We think these differences may be explained by the three-dimensional distribution of the Alfvén speed. We will study the three-dimensional

TABLE 1
ESTIMATED FAST-SHOCK SPEED v_{sh}

Parameter	$B_1/B_{p1} = 1/3^a$			$B_1/B_{p1} = 1/2$		
	B_1 (G)	2.66	2.66	2.66	3.99	3.99
T_1 (MK)	2.00	2.25	2.50	2.00	2.25	2.50
EM_1^b (cm $^{-5}$)	$10^{27.3}$	$10^{27.0}$	$10^{26.9}$	$10^{27.3}$	$10^{27.0}$	$10^{26.9}$
n_1 (cm $^{-3}$)	$10^{8.7}$	$10^{8.5}$	$10^{8.4}$	$10^{8.7}$	$10^{8.5}$	$10^{8.4}$
v_{A1} (km s $^{-1}$)	274	328	369	411	492	553
c_{s1} (km s $^{-1}$)	215	228	240	215	228	240
$\theta_1 = 90^\circ$						
T_2 (MK)	2.33	2.75	3.16	2.34	2.77	3.19
X	1.25	1.32	1.36	1.24	1.31	1.35
v_{sh} (km s $^{-1}$)	410	493	559	546	668	761
M_f^c	1.18	1.23	1.27	1.18	1.23	1.26
$\theta_1 = 60^\circ$						
T_2 (MK)	2.33	2.75	3.16	2.34	2.78	3.20
X	1.24	1.32	1.36	1.24	1.30	1.34
v_{sh} (km s $^{-1}$)	397	478	542	533	653	745
M_f^c	1.14	1.20	1.23	1.15	1.20	1.24

NOTE.— $\theta_1 = 90^\circ$ means perpendicular shock, and $\theta_1 = 60^\circ$ oblique.

^a B_{p1} is the photospheric magnetic field strength.

^b $EM_1 = n_1^2 l$, where l is the line-of-sight length, which is assumed equal to the pressure scale height of the corona.

^c M_f is fast-mode Mach number.

structure of the propagation of the coronal shock with more observed data and will simulate the flare-associated coronal wave in our future work.

From the above analysis, we can estimate the coronal plasma velocity just behind the Moreton wave (fast-mode MHD shock), $v_1 - v_2$, to be about 100–200 km s $^{-1}$, which would be observed at 50–100 km s $^{-1}$ along the line of sight with the *SOHO*/Coronal Diagnostics Spectrometer or the *Solar-B*/EUV Imaging Spectrometer.

Our result, $M_f = 1.15$ – 1.25 , indicates that the propagation speed of the Moreton wave is comparable to the MHD fast-

mode speed and consistent with Uchida's model of a weak MHD fast-mode shock. On the other hand, Wang (2000) showed that the propagation speed of an EIT wave is comparable to the coronal MHD fast-mode speed and suggested that the Moreton wave may be associated with a highly super-Alfvénic shock. This seems inconsistent with our result. But if we assume that the Alfvén (and the fast-mode) velocity is increasing with height in the low corona (Mann et al. 1999), and that X-ray waves and EIT waves are propagating at two different heights, Wang's suggestion may not be in contradiction to our results.

The fitting lines for the Moreton wave and X-ray wave in Figure 2 suggest that the start time of these waves may be somewhat earlier than the flare. This is curious since Moreton waves usually occur with flares. It may be explained by the deceleration of the Moreton wave as seen in Figure 2. This is in accordance with the results of Warmuth et al. (2001) and implies that the initial velocities of the Moreton wave and probably also the X-ray wave were actually higher than the mean values we found; i.e., the shock may be stronger in the early phase.

Finally, we note that an EIT wave and a type II radio burst were also observed simultaneously with this Moreton wave. The relationship between the EIT wave and the Moreton wave will be studied in our future paper (N. Narukage et al. 2002, in preparation).

The authors thank S. Eto, H. Isobe, A. Asai, H. Kozu, T. T. Ishii, and M. Kadota for useful discussions. The *Yohkoh* satellite is a Japanese national project, launched and operated by ISAS, and involving many domestic institutions, with multi-lateral international collaboration with the US and the UK. *SOHO* is a mission of international cooperation between the European Space Agency and NASA. This work was supported in part by the JSPS Japan-US Cooperation Science Program (principal investigators: K. Shibata and K. I. Nishikawa).

APPENDIX

In this Letter, we estimated the fast-shock speed ($v_{sh} = v_{1x} = v_1 \cos \theta_1$) by assuming the coronal magnetic field strength, $B_1 = (\frac{1}{3}$ or $\frac{1}{2})B_{p1}$, and found that v_{sh} is comparable to the observed X-ray wave speed, confirming that the X-ray wave is an MHD fast-mode shock. However, we can take a different approach; it is possible to estimate the coronal magnetic field strength, if we use the observed X-ray wave propagation speed and the MHD shock theory (eqs. [1]–[7]), since $(I_{X1}, T_1, \theta_1, v_1, I_{X2})$ determines $(B_1, T_2, B_2, \theta_2, v_2)$. Figure 3 shows the estimated fast shock speed as a function of B_1/B_{p1} on the basis of equations (1)–(7). From this figure and the observed propagation speed of the X-ray wave, 630 ± 100 km s $^{-1}$, we can estimate B_1/B_{p1} to be 0.3–0.7. This value seems to be consistent with the calculated coronal magnetic field strength using source-surface field extrapolations (e.g., Dere 1996; Wang 2000). Hence, this approach also confirms that the X-ray wave is an MHD fast-mode shock.

REFERENCES

- Dere, K. P. 1996, *ApJ*, 472, 864
Eto, S., et al. 2002, *PASJ*, in press
Kai, K. 1969, *Sol. Phys.*, 10, 460
Khan, J. I., & Aurass, H. 2002, *A&A*, 383, 1018
Khan, J. I., & Hudson, H. S. 2000, *Geophys. Res. Lett.*, 27, 1083
Klassen, A., Aurass, H., Mann, G., & Thompson, B. J. 2000, *A&AS*, 141, 357
Kurokawa, H., et al. 1995, *Geomag. Geoelectr.*, 47, 1043
Mann, G., Klassen, A., Estel, C., & Thompson B. J. 1999, in *Proc. Eighth SOHO Workshop, Plasma Dynamics and Diagnostics in the Solar Transition Region and Corona*, ed. J.-C. Vial & B. Kaldeich-Schumann (ESA SP-446; Noordwijk: ESA), 477
Moreton, G. E. 1960, *AJ*, 65, 494
Priest, E. R. 1982, *Solar Magnetohydrodynamics* (Dordrecht: Reidel), chap. 5.4
Scherrer, P. H., et al. 1995, *Sol. Phys.*, 162, 129
Smith, S. F., & Harvey, K. L. 1971, in *Physics of the Solar Corona*, ed. C. J. Macris (Dordrecht: Reidel), 156
Thompson, B. J., et al. 2000, *Sol. Phys.*, 193, 161
Tsuneta, S., et al. 1991, *Sol. Phys.*, 136, 37
Uchida, Y. 1968, *Sol. Phys.*, 4, 30
———. 1970, *PASJ*, 22, 341
Uchida, Y., Altschuler, M. D., & Newkirk, G., Jr. 1973, *Sol. Phys.*, 28, 495
Wang, Y. M. 2000, *ApJ*, 543, L89
Warmuth, A., Vrsnak, B., Aurass, H., & Hanslmeier, A. 2001, *ApJ*, 560, L105